Seasonal cycle of variability, instabilities, and subduction at submesoscales

Zachary K Erickson,*[1] Andrew F Thompson,[1] Jörn Callies,[1] and Patrice Klein[2]

[1]Caltech, Division of Geological and Planetary Sciences; Pasadena, CA [2]Caltech, Jet Propulsion Laboratory; Pasadena, CA

*Contact: zerickso@caltech.edu | PDF: http://web.gps.caltech.edu/~zerickso/Posters/OCB18.pdf

Key points

- Observational[1,2] and high-resolution (1/48°) model[3] data explore the impact and seasonality of submesoscale processes in the upper 1 km of the open ocean.
- 5 ocean gliders were deployed in a small region of the northeast Atlantic (20 × 20 km) for a year.[1,2]
- Potential energy (PE) increases in winter at depths much greater than the mixed layer depth (MLD), suggesting exchange of water across the base of the mixed layer during winter.
- Slopes of PE and spice structure function are s^1, consistent with a spectral slope of k^{-2}.
- Weak stratification across the base of the mixed layer in winter leads to higher potential for subduction of water and biological export.

See:
· *Erickson and Thompson, GBC, The seasonality of physically-driven export at submesoscales in the northeast Atlantic Ocean, in revision.*
· *Erickson, Thompson, Callies, and Klein, The vertical structure of submesoscale variability during a full seasonal cycle, in prep.*

Study Site

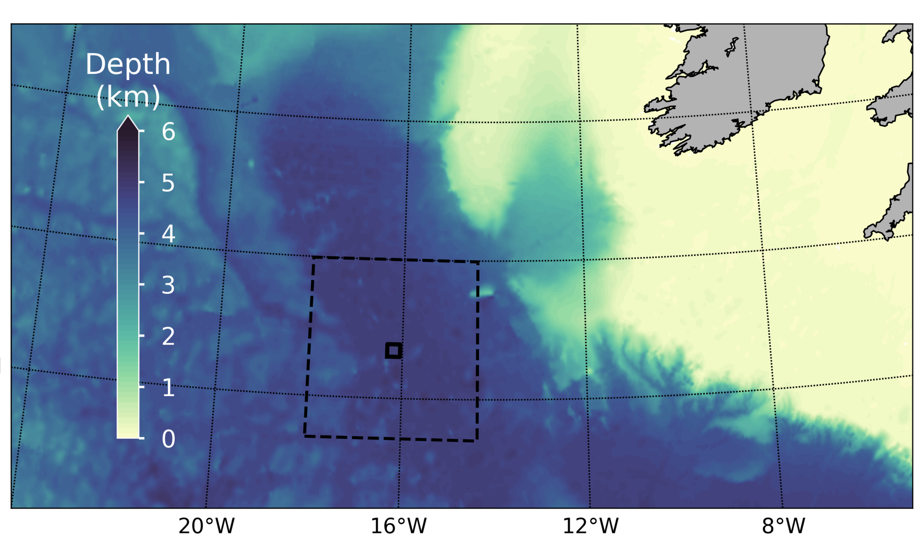

Figure 1: Glider (solid) and model (dotted) region.

Structure Functions

Structure functions are a complementary approach to Fourier power spectra, and are useful for simultaneous glider deployments.

$$D_\Pi(s) = \overline{[\Pi(\mathbf{x}) - \Pi(\mathbf{x}+s)]^2}^{\mathbf{x},t}$$

Structure functions slope s^γ is related to a spectral slope $k^{-\lambda}$ as:[4]

$$\lambda = \gamma + 1$$

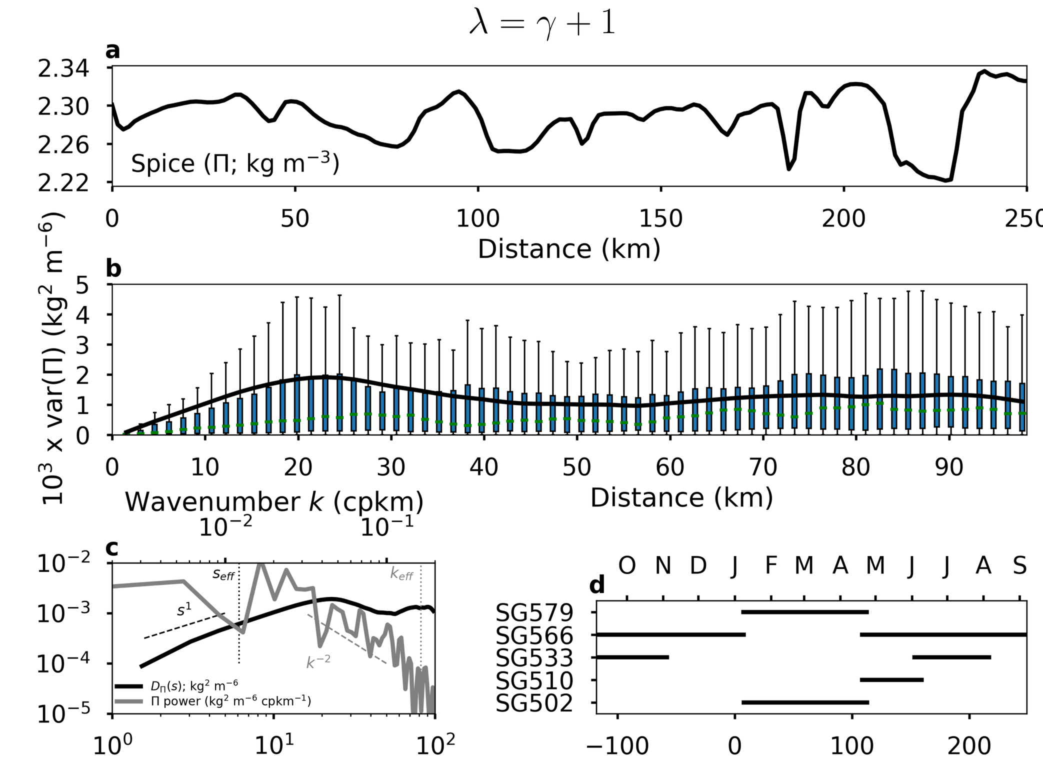

Figure 2: **(a)** Sample spice along a given latitude from a model snapshot. **(b)** Structure function of the data (black). Box-plots showing median (green line), interquartile range (blue rectangle), and full range of variability (error bars) at each s. **(c)** Comparison of the structure function $D_\Pi(s)$ (black) with a Fourier power spectrum for the same dataset (grey). Effective resolution is shown as $4\Delta x$, where $\Delta x \approx 1.5$ km. **(d)** Black lines denote time when each glider was deployed.

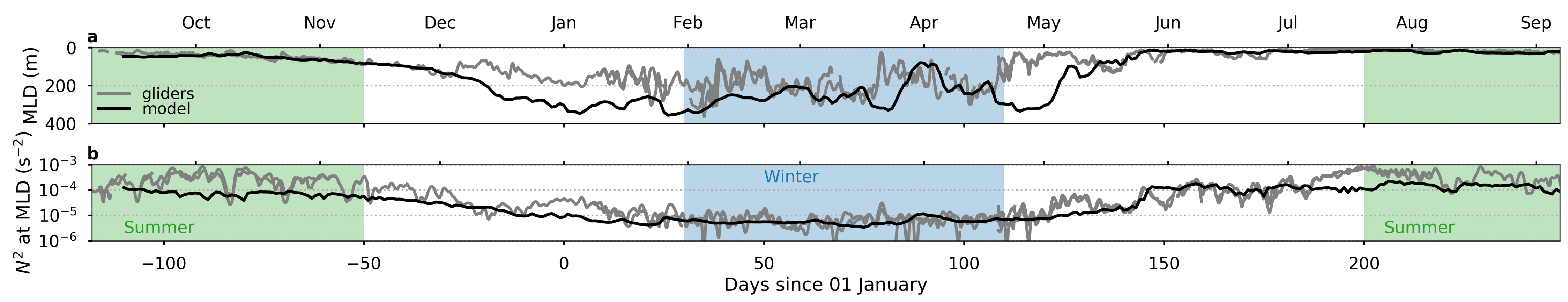

Figure 3: **(a)** MLD for the gliders (black) and model (grey), defined as $\Delta\sigma = 0.03$ kg/m^3 from σ_{ref} at 10 m depth. **(b)** $N^2 = b_z$ at the base of the mixed layer.

Winter

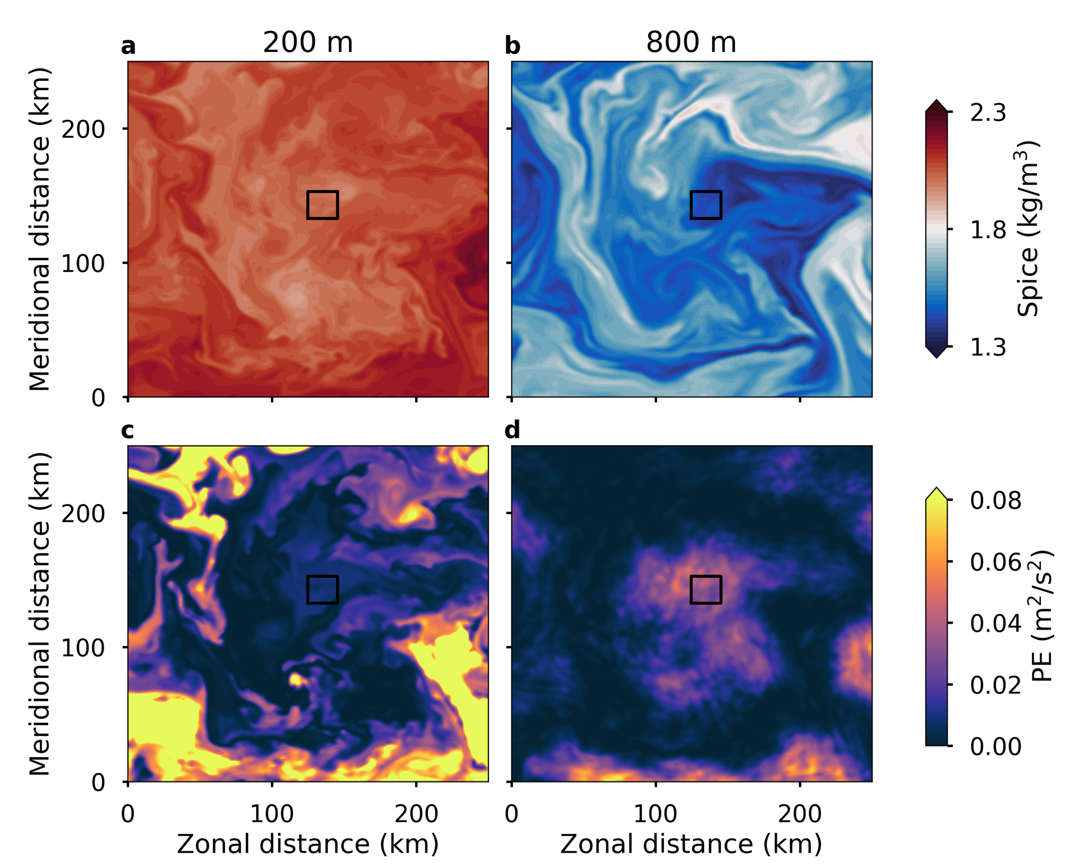

Figure 4: Spice **(a,b)** and potential energy PE $= \frac{1}{2}b'^2/b_z$ **(c,d)** at 200 m **(a,c)** and 800 m **(b,d)** depth from a model snapshot on 01 January 2012. Black box in each panel gives the size of the glider deployment region. Spice is plotted along constant potential density surfaces corresponding to each depth ($\sigma = 27.08$ and 27.45 kg/m^3, respectively), to negate effects of internal waves.

- Wintertime MLD varies from about 100–350 m.
- Spice gradients are small due to efficient mixing during winter.
- High PE in mixed layer vs. at depth.
- Increase in PE and low spice variability at all scales deeper than the maximum MLD suggests increased exchange across the ML base.
- Oxygen variability varies with depth but not with spatial scale.

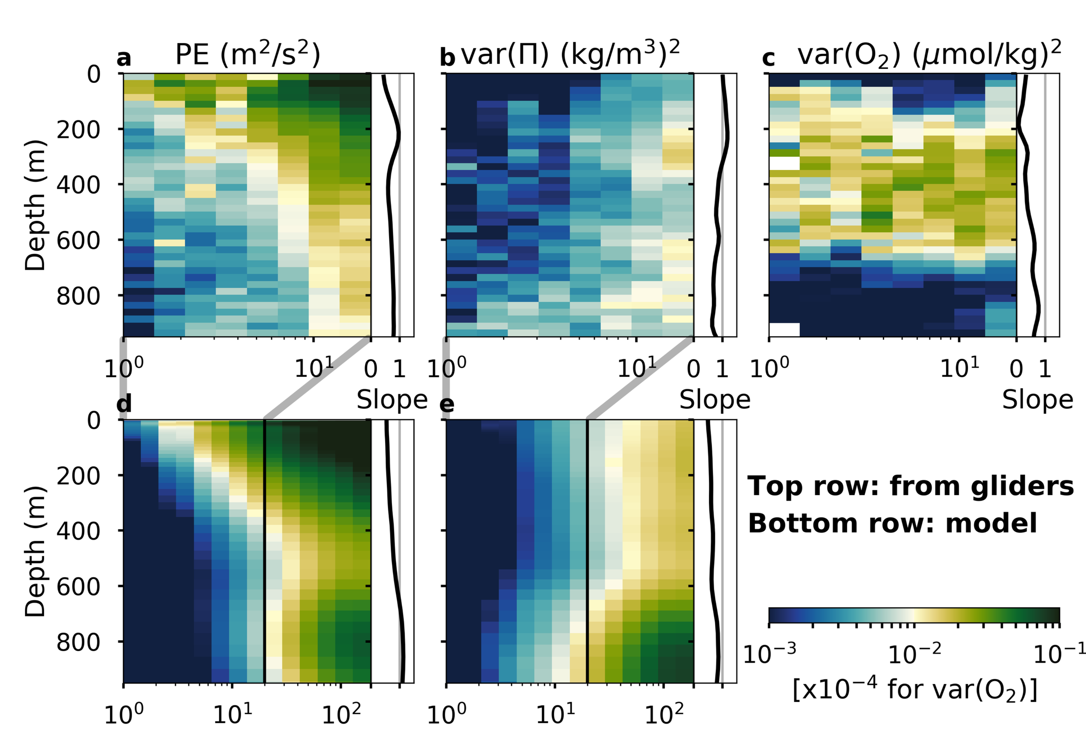

Figure 5: Structure functions during winter measurements (31 Jan to 10 Nov) for potential energy ($\frac{1}{2}D_b(s)/\overline{b_z}$) **(a,d)**, spice (Π) **(b,e)**, and oxygen **(c)** for gliders **(a-c)** and model **(d,e)**. Best-fit log-log slopes (γ) for each depth are shown on the right **(a-e)**.

Summer

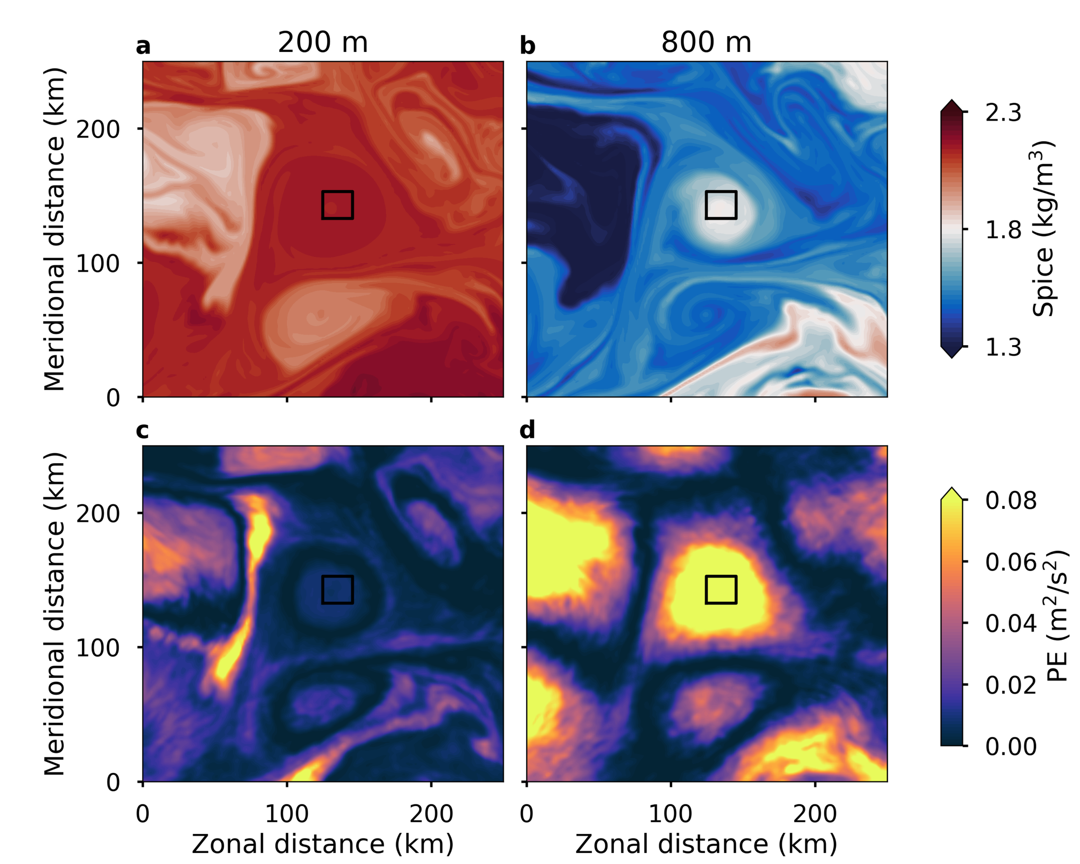

Figure 6: Spice **(a,b)** and potential energy PE $= \frac{1}{2}b'^2/b_z$ **(c,d)** at 200 m **(a,c)** and 800 m **(b,d)** depth from a model snapshot on 01 September 2012. Black box in each panel gives the size of the glider deployment region. Spice is plotted along constant potential density surfaces corresponding to each depth ($\sigma = 27.11$ and 27.43 kg/m^3, respectively), to negate effects of internal waves.

- Summertime MLD < 100 m.
- Spice gradients are large due to inefficient mixing during summer.
- Higher PE at depth than just below mixed layer.
- Sharp distinction in PE and spice variability at MLD, suggesting rigid boundary at the base of the mixed layer in summer
- Oxygen variability varies with depth and with spatial scale.

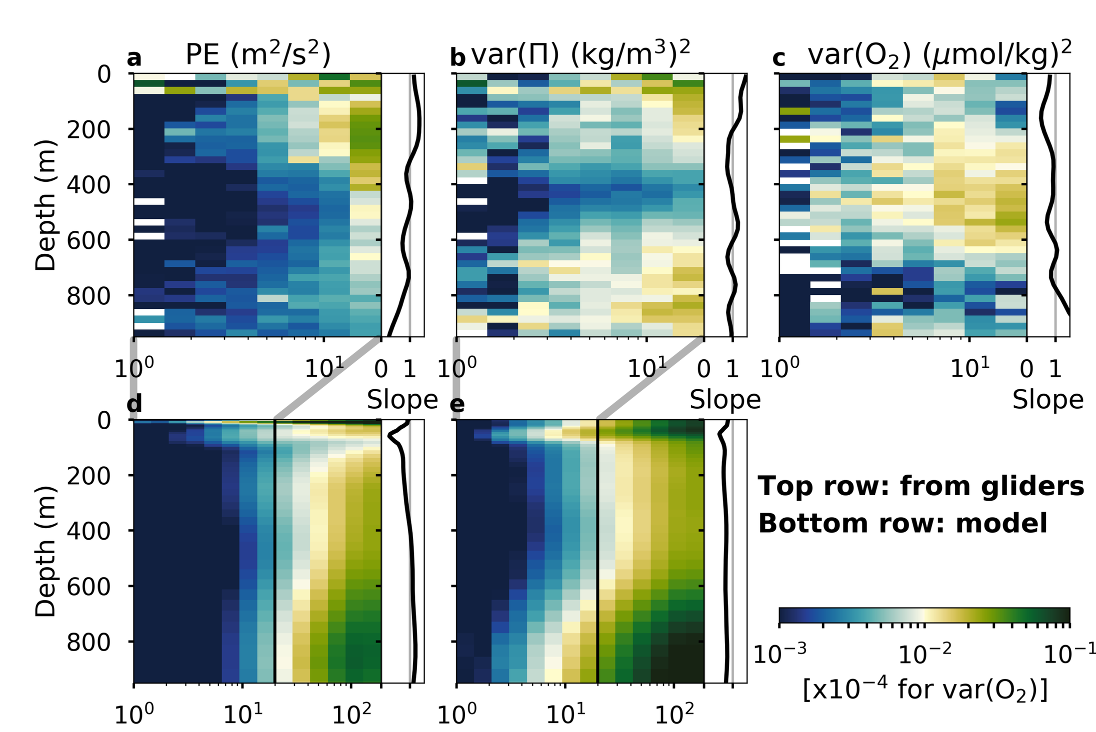

Figure 7: Structure functions during winter measurements (18 Jul to 19 Apr) for potential energy ($\frac{1}{2}D_b(s)/\overline{b_z}$) **(a,d)**, spice (Π) **(b,e)**, and oxygen **(c)** for gliders **(a-c)** and model **(d,e)**. Best-fit log-log slopes (γ) for each depth are shown on the right **(a-e)**.

[1] Thompson, A. F. et al. (2016), *J. Phys. Oc.*, **46**, 1285-1307.
[2] Damerell, G. M. et al. (2016), *J. Geophys. Res., Oc.*, **121**, 3075-3089.
[3] Menemenlis, D. et al. (2008), *Merc. Oc. Quart. News.*, **31**, 13-21.
[4] McCaffrey, K. et al. (2013), *J. Phys. Oc.*, **45**, 1773-1793.
[5] Thomas, L. N. et al. (2013), *Deep-Sea Res. II*, **91**, 96-110.
[6] Fox-Kemper, B. et al. (2008), *J. Phys. Oc.*, **38**, 1145-1165.

Implications for biological export

Biological export through submesoscale instabilities requires these instabilities to be co-located with biological material (e.g. particulate organic carbon; POC) in the surface ocean. The two major instabilities considered here are symmetric instability (SI) and baroclinic mixed layer instability (MLI). SI acts to the maximum depth H such that[5]

$$f\int_0^H \mathrm{PV}\mathrm{d}z < 0,$$

for PV $= (f + v_x - u_y)b_z + u_z b_y - v_z b_x$. For glider data, we approximate[1] PV $\approx (f + v_x)b_z - b_x^2/f$. Vertical velocity associated with MLI can be estimated from an overturning streamfunction:[6]

$$w = \psi_x; \qquad \psi = 0.06\frac{\mu(z) b_x \mathrm{MLD}^2}{|f|}.$$

The normalized function $\mu(z)$ represents the strength of the overturning throughout the mixed layer and is set to 1, giving a maximum w.

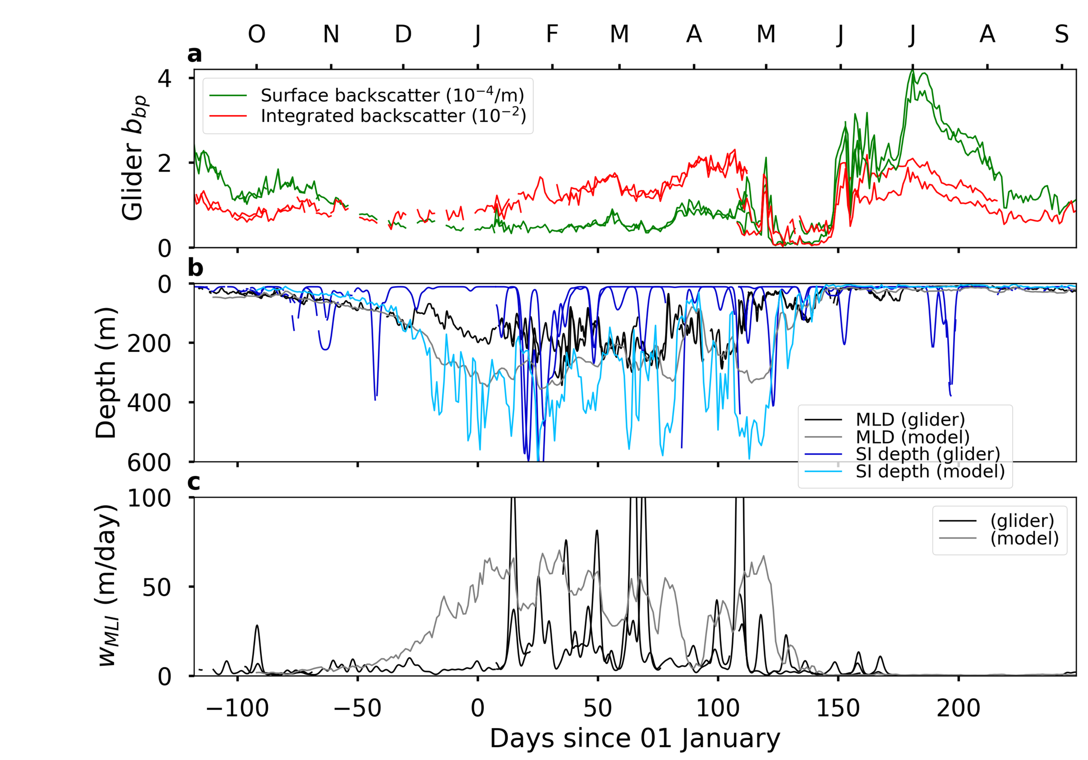

Figure 8: **(a)** Particulate backscatter (b_{bp}) as an average over the upper 25 m (green) and integrated over the upper 500 m (red) from glider measurements. **(b)** MLD from gliders (black) and model (grey). Depth at which symmetric instability (SI) acts in dark blue (gliders) and light blue (model). **(c)** Derived absolute value of vertical velocities associated with mixed layer baroclinic instabilities from the glider data (black) and model (grey). For all panels, glider data are averaged using a Gaussian filter with standard deviation of one day, and model data are averaged over the dotted region in Figure 1.

- Subduction by SI and MLI is enhanced during winter and early spring.
- Biological production is enhanced in spring and summer (although some indication of larger POC concentrations during winter).
- Export production through submesoscale instabilities most likely during spring.

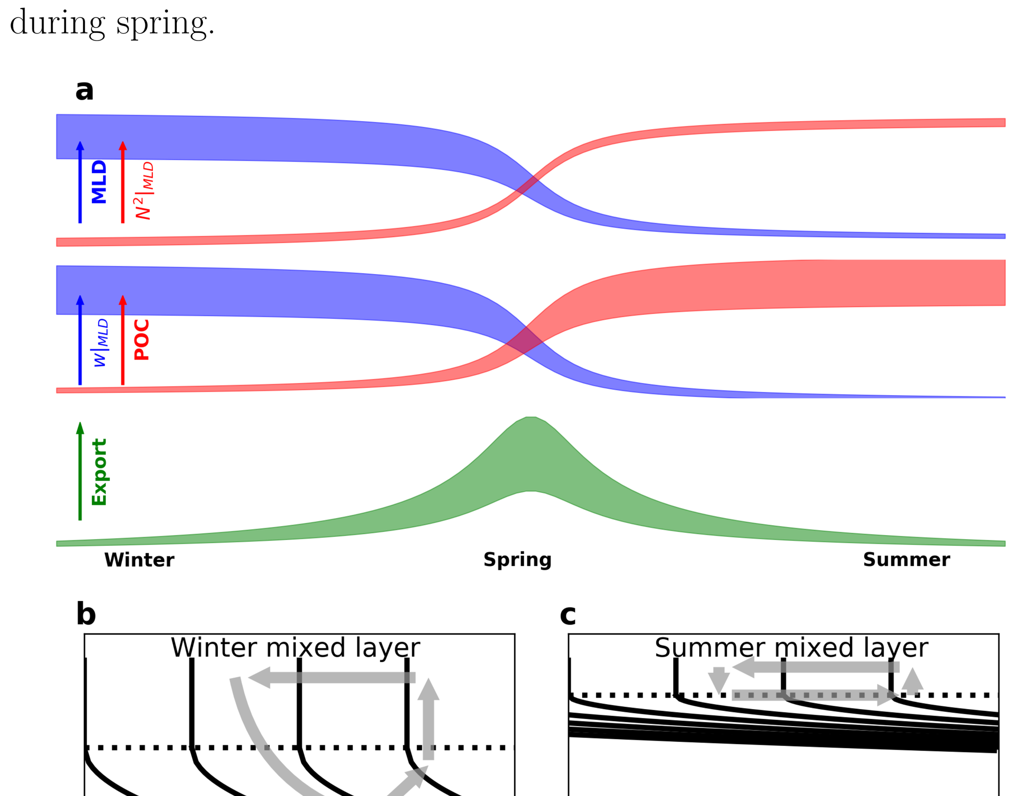

Figure 9: **(a)** Schematic of the seasonal evolution of the MLD, the strength of the pycnocline (N^2 at base of mixed layer), the strength of vertical motions associated with submesoscale instabilities (w at base of the mixed layer), particulate organic carbon (POC) concentrations, and export $\langle w'\mathrm{POC}'\rangle$ throughout the year. **(b,c)** Schematics for winter and summer surface ocean densities, where solid lines are isopycnal surfaces, dotted lines are the MLDs, and grey arrows show the effect of baroclinic mixed layer instabilities.